

Multi-defect microscopy image restoration under limited data

Anastasia Razdaibiedina, Jeevaa Velayutham, Miti Modi



Background

Degradation of fluorescence microscopy images occurs due to many factors, including bleaching of fluorophores, readout noise from sensors, out-of-focus light, poor axial sampling, and uneven illumination and detection. In this work, we focus on three common tasks in microscopy image restoration:

- Denoising
- Axial inpainting
- Deep learning enabled super-resolution.

We used three publicly available datasets, which represent the above-mentioned defect types:

Organism	Biological Structure	Restoration task	average PSNR / SSIM
Drosophila	whole embryo	denoising	19.92 / 0.63
Zebrafish	retinal nuclei	axial inpainting	12.51 / 0.33
Human	HeLa cells microtubules	super-resolving	7.27 / 0.08

Table 1: Description of datasets used for the experiments. PSNR / SSIM column denotes average PSNR and SSIM scores across the whole dataset before image reconstruction.

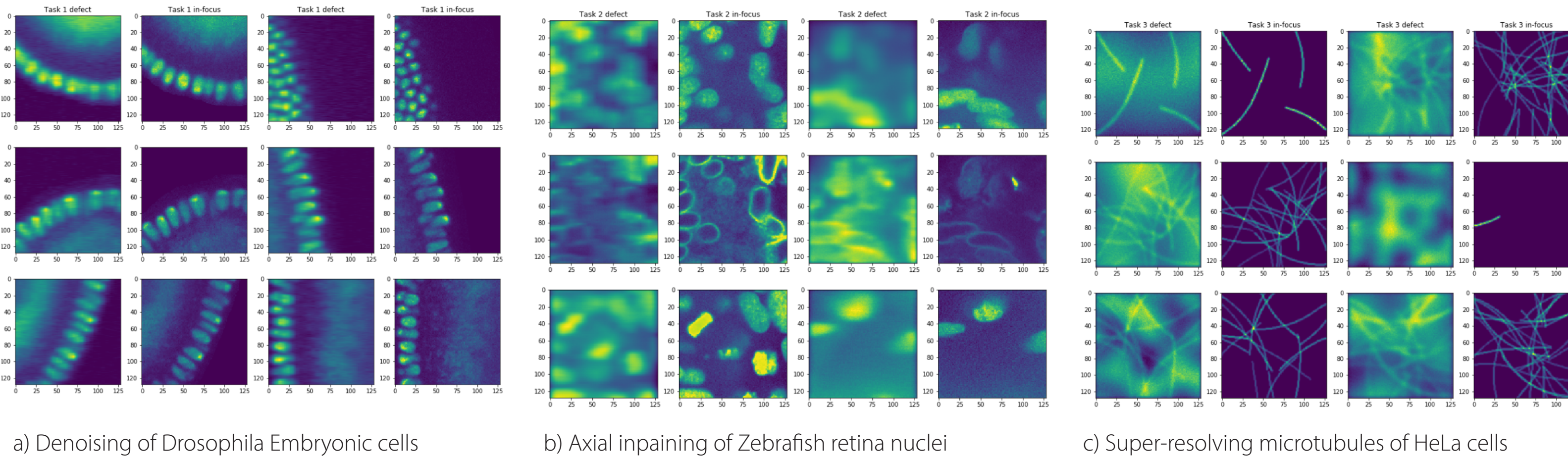
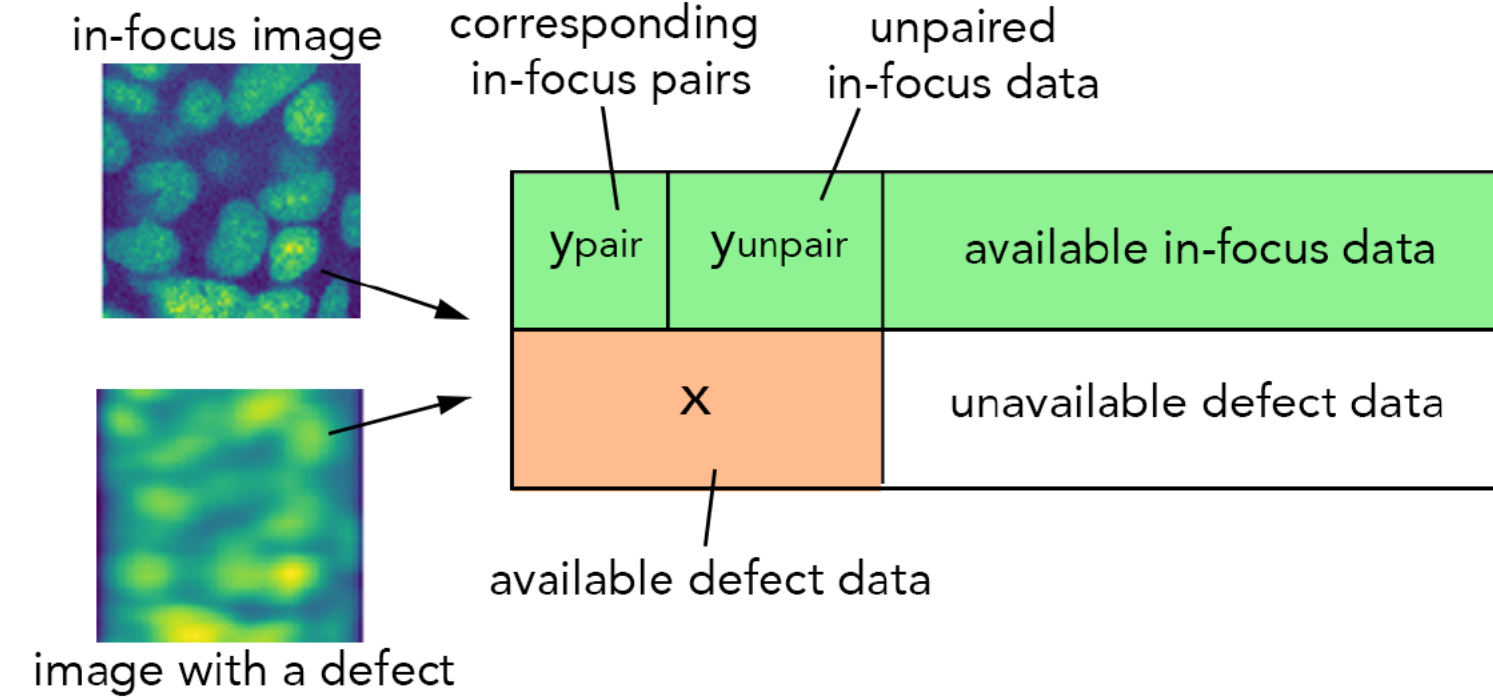


Figure 1: Examples of micrograph dataset used for experiments.

Objective

We propose a unified method for multi-defect micrograph restoration. To overcome the problem of limited training data, which is a common challenge for experimental databases, we incorporate meta-learning style data augmentation into our pipeline.



Method

Generative Adversarial Networks (GANs)

The generator G and the discriminator D play a minimax game where the generator is trained to maximize the probability of discriminator making an error:

$$\min_{G} \max_{D} \mathbb{E}_{x \sim \mathbb{P}_r} [\log(D(x))] + \mathbb{E}_{z \sim \mathbb{P}_z} [\log(1 - D(G(z)))]$$

where \mathbb{P}_r is the real data distribution and \mathbb{P}_z is the model distribution.

Proposed 2-step approach: augment data with CIN-GAN + train conditional GAN to do the restoration.

1) CIN-GAN for data augmentation

CIN-GAN is inspired by Conditional Instance Normalization (CIN) commonly used for style transfer. All layers of this GAN are shared by different defect types except for the CIN layers. These CIN layers are turned on/off depending on the type of defect that being synthesized. CIN layer is defined as:

$$z = \gamma_i \left(\frac{x - \mu}{\sigma} \right) + \beta_i$$

where i = number of tasks, μ = mean of input x , σ = standard deviation of input x , γ and β are separately learned parameters for each task. We apply condition on the instance normalization for each defect type.

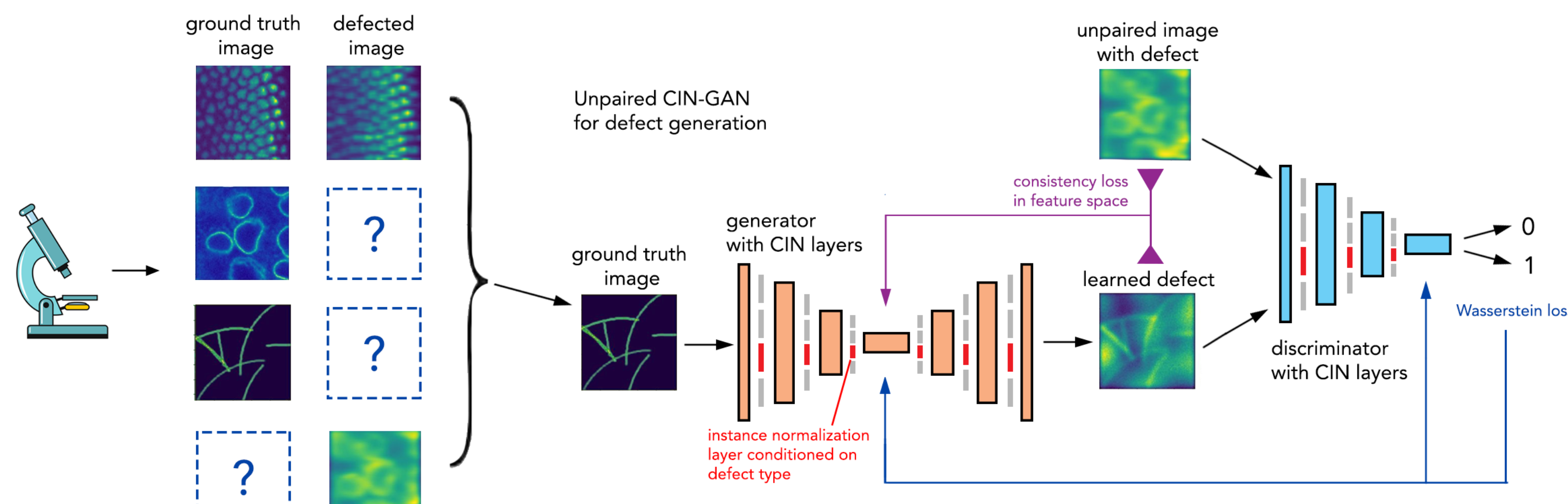


Figure 2a: Illustration of the proposed pipeline. GAN with conditional instance normalization (CIN) layers for generating different microscopy defects. Since paired data is often unavailable, CIN-GAN is trained on a small amount of unpaired defective and ground truth microscopy image data; different CIN layers are "switched" on / off depending on the task.

Since CIN-GAN is trained on unpaired data, we used Wasserstein loss as adversarial loss for this model to overcome the saturation problem by providing a meaningful gradient signal throughout the training:

$$\min_{G} \max_{w \in W} \mathbb{E}_{x \sim \mathbb{P}_r} [f_w(x)] - \mathbb{E}_{z \sim \mathbb{P}_z} [f_w(G(z))]$$

Total total loss of CIN-GAN also includes style loss and content loss: $\mathcal{L} = \lambda_a \mathcal{L}_{adv} + \lambda_c \mathcal{L}_{content} + \lambda_s \mathcal{L}_{style}$

$$\mathcal{L}_{content} = \sum_{i \in C} \frac{1}{U_i} \|\phi_i(x) - \phi_i(\hat{x})\|_2^2 \quad \mathcal{L}_{style} = \sum_{i \in S} \frac{1}{U_i} \|\mathcal{G}(\phi_i(x)) - \mathcal{G}(\phi_i(\hat{x}))\|_F^2$$

Style loss ensures that two images will be similar in style if the difference between Gram matrices of low-level features of the images extracted from a pretrained classifier has small Frobenius norm. Content loss ensures that two images are similar in content by making the high level features extracted from a pretrained classifier closer in the Euclidean space.

2) cGAN

After the dataset is augmented by CIN-GAN, a conditional GAN is trained on paired high-resolution ground-truth images and defective images. The resulting cGAN is used to restore multiple types of microscopy defects

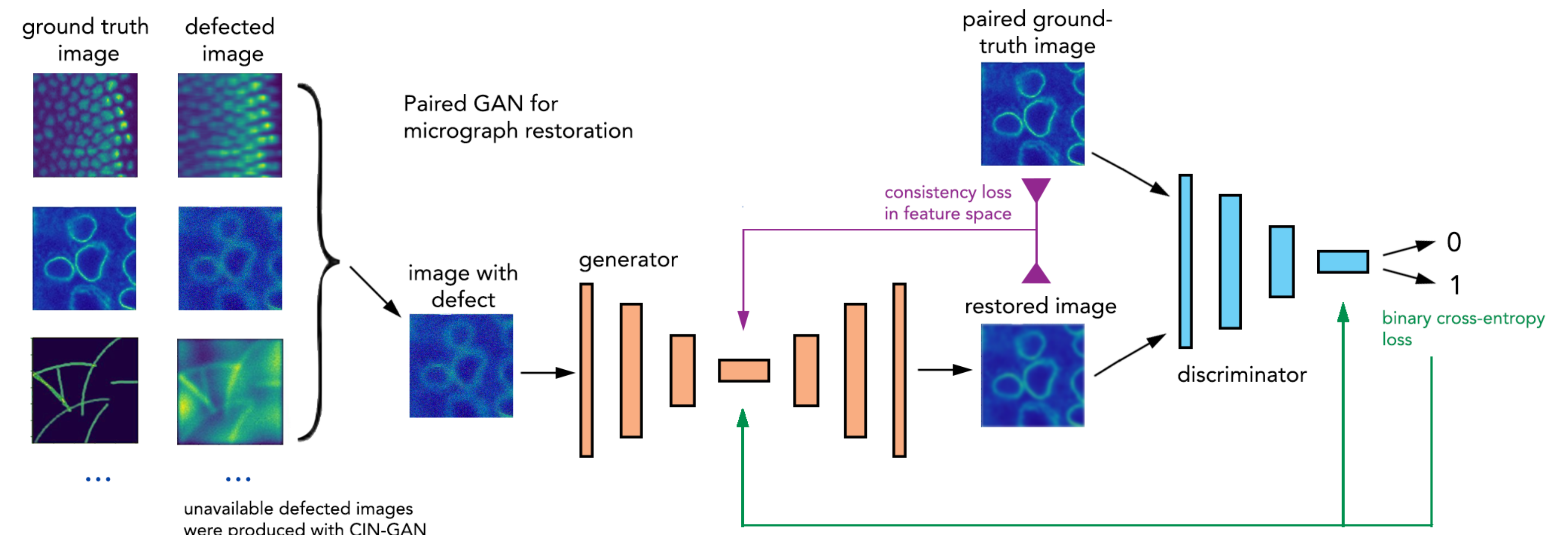


Figure 2b: Illustration of the proposed pipeline. Conditional GAN trained on paired ground truth + defected image data for subsequent data restoration.

The total loss function of cGAN is:

$$L_{total} = L_{adv} + \lambda \cdot L_{content}$$

where adversarial loss is cross-entropy loss (we didn't need Wasserstein loss due to similarities of input and output distributions).

Results

We compared performance of our restoration pipeline in two settings:

A) Limited amount of real paired images (defective + in-focus)

B) No real pairs are available, and all defective pairs for cGAN training were synthetically generated.

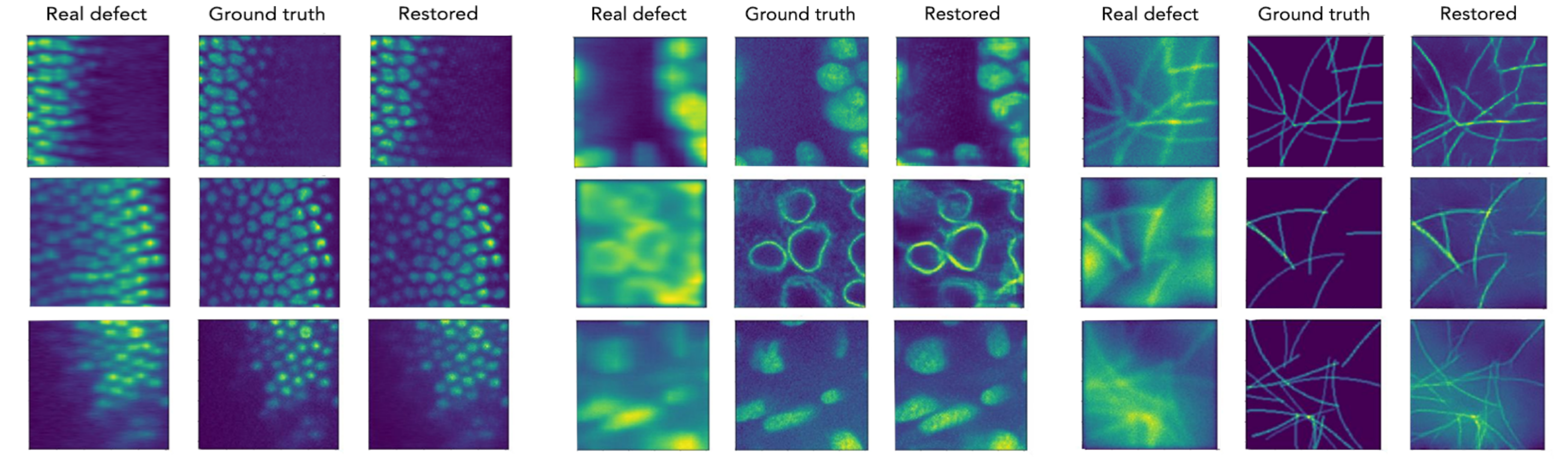


Figure 3: Examples of micrographs restoration with the proposed pipeline on three distinct tasks. 10 real pairs of images were used for training; dataset was augmented with CIN-GAN.

	Denoising	Axial inpainting	Super-resolution
CARE	21.6/ 0.56	12.8/0.29	14.1/0.20
DeblurGAN	18.0/0.33	14.6/0.20	11.2/0.14
Ours	22.4/0.56	17.4/0.38	14.3/0.22
CycleGAN	21.3/0.49	15.3/0.27	12.7/0.14
Ours	21.9/0.57	15.1/0.32	8.9/0.07

Table 2: Comparison of PSNR / SSIM scores between our cGAN restoration network with other models with 10 paired images (top) or no paired data (bottom)

A) For the paired setting, we compared our model performance with two existing state-of-the-art image restoration models: DeblurGAN and U-Net based CARE models.

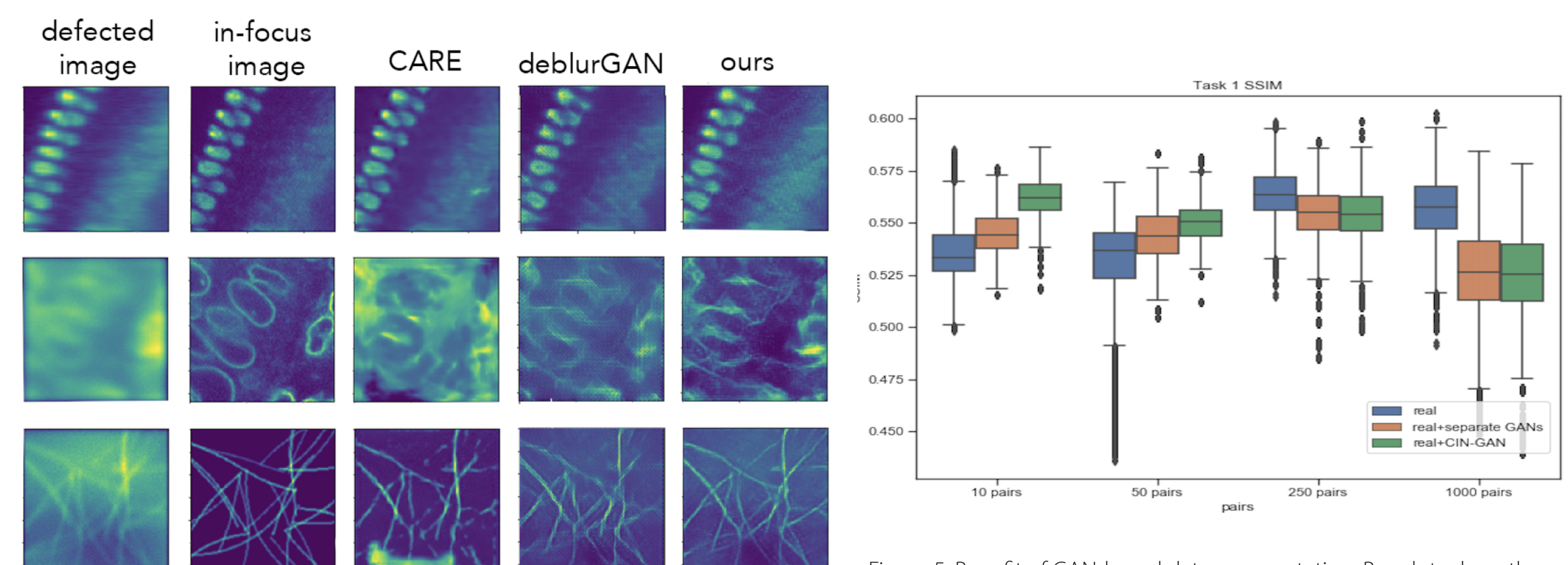


Figure 4: Comparison of three paired image restoration pipeline on 10 paired images ($|x| = 10, |y_{paired}| = 10$ for each task)

B) For the unpaired setting we assumed that real paired training data was not available. CIN-GAN was used to generate artificial defects to create paired training data for cGAN which restores the real defective images. We compare this performance with state-of-the-art unpaired image to image translation model, CycleGAN.

Is it beneficial to use unified model?

Under limited data settings, our unified model (CIN-GAN + cGAN) outperforms separately trained GANs (Figure 5).

Can we generate distinct defects with one CIN-GAN?

Figures 5 and 6 confirm CIN-GAN's capability to synthesize distinct artifacts shown visually and through divergence in PSNR scores.

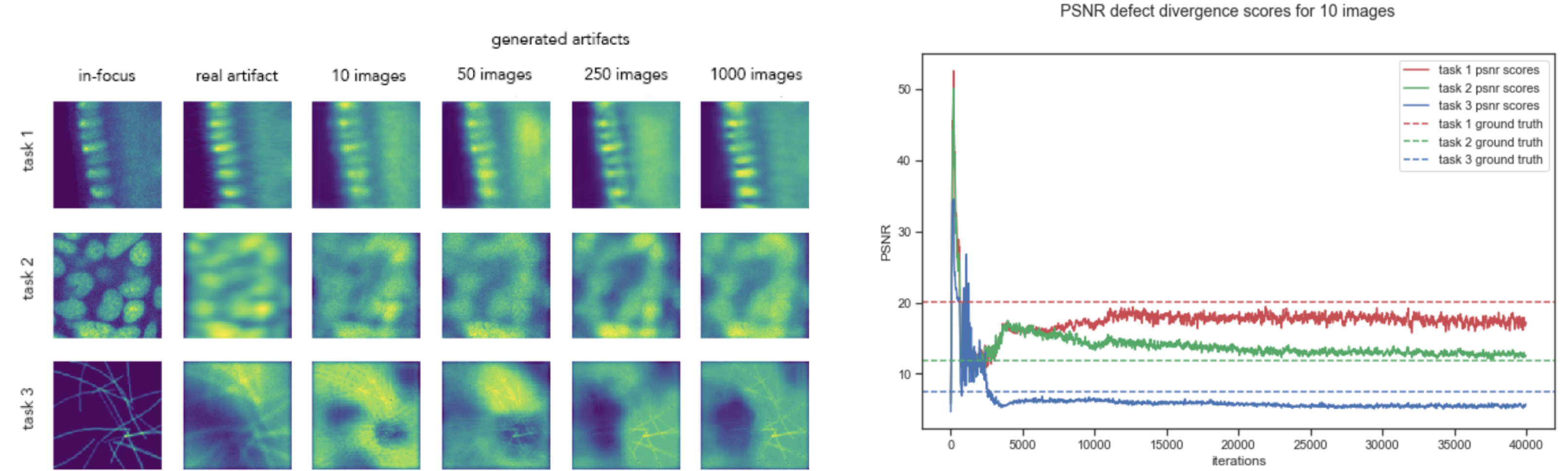


Figure 5: Benefit of GAN-based data augmentation. Boxplots show the distribution of PSNR scores for restored images for real paired data, real data augmented by separate GANs and real data augmented by CIN-GAN. Plots are shown for 10, 50, 250 and 1000 data pairs. CIN-GAN data augmentation proves to be beneficial in cases when limited paired data is available.

Figure 6: Results of CIN-GAN aided artifact generation for three defected tasks using 10, 50, 250, and 1000 unpaired defect images.

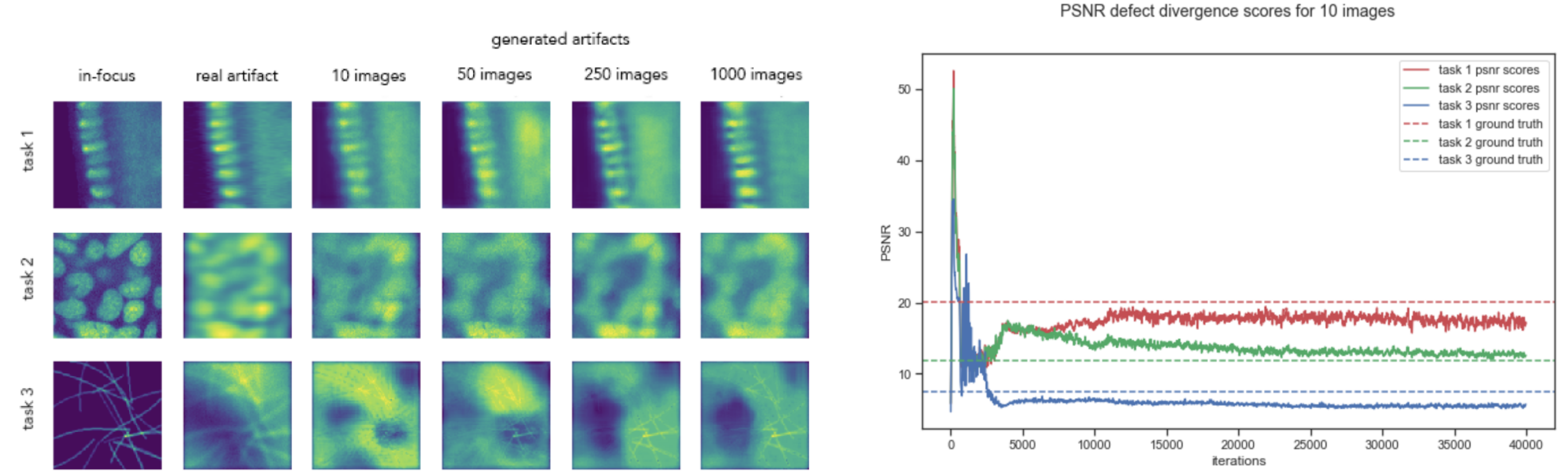


Figure 7: Learning to realistically generate discrete artifacts with CIN-GAN. The plot shows divergence score progression over training time, measured as PSNR of in-focus and artificially generated defective images. Dashed lines represent the ground truth PSNR divergence score between in-focus and real defect.